

THE BAIE-DES-MOUTONS SYENITIC COMPLEX, LA TABATIÈRE, QUÉBEC I. PETROGRAPHY AND FELDSPAR MINERALOGY

ANDRÉ E. LALONDE AND ROBERT F. MARTIN

Department of Geological Sciences, McGill University, 3450 University Street,
Montreal, Quebec H3A 2A7

ABSTRACT

The early Cambrian syenitic complex of Baie-des-Moutons, La Tabatière, Québec, consists of thirteen distinct petrographic rock-units arranged in three intrusive groups, here called *early*, *intermediate* and *late*. The feldspars in these thirteen cone-sheets have re-equilibrated deuterically to various extents. The turbid appearance of feldspars from most units results from an increase in the abundance of fluid inclusions. The postmagmatic development of these inclusions is accompanied by 1) increase in Al-Si order, 2) coarsening of exsolution textures, 3) nucleation of strain-free domains and 4) crystallization of hydrous alteration minerals; all suggest recrystallization, possibly not strictly isochemical, in the presence of an aqueous volatile phase. Feldspar oxygen-isotope ratios demonstrate the magmatic nature of this volatile phase. In some rock-units, this recrystallization process is incipiently developed and restricted to phenocryst rims and transecting fractures. The pink coloration of feldspars, due to the presence of hematite flakes on the walls of the fluid inclusions, reflects oxidizing conditions during recrystallization. Na- and K-feldspars of the intermediate-group syenites are better ordered than their early- and late-group counterparts, a reflection of bulk-rock alkalinity.

Keywords: syenite, feldspar, postmagmatic re-equilibration, Al-Si order, perthite, oxygen-isotope ratio, hematite, Baie-des-Moutons, Quebec, St. Lawrence rift.

SOMMAIRE

Le complexe syénitique de Baie-des-Moutons, La Tabatière (Québec), d'âge Cambrien inférieur, comporte treize unités pétrographiques distinctes mises en place en trois cycles intrusifs, que nous appelons *précoce*, *intermédiaire* et *tardif*. Les feldspaths, dans ces treize unités en feuillet conique, ont ré-équilibré à divers degrés au stade deutérique. La turbidité du feldspath dans la plupart des unités reflète une augmentation du nombre des inclusions fluides. Les phénomènes suivants accompagnent le développement de ces inclusions à un stade post-magmatique: 1) augmentation dans le degré d'ordre Al-Si, 2) augmentation de la taille des grains dans la texture d'exsolution, 3) nucléation de do-

maines non contraints et 4) cristallisation de minéraux d'altération hydratés. Tous ces phénomènes indiqueraient une recristallisation, non rigoureusement isochimique, en présence d'une phase volatile aqueuse. Les valeurs du rapport d'isotopes d'oxygène, déterminé sur cristaux de feldspaths, indiquent l'origine magmatique de cette phase gazeuse. Dans certaines unités, le processus de recristallisation n'est qu'incipient, limité surtout à la bordure des phénocristaux et le long de fractures qui les recourent. La coloration rose des feldspaths, qui est due à la présence de cristaux d'hématite sur les parois des inclusions fluides, témoigne de l'oxydation pendant la recristallisation. Les feldspaths sodique et potassique des syénites du cycle intermédiaire sont mieux ordonnés que leurs analogues des cycles précoce et tardif à cause de la plus grande alcalinité de la roche.

Mots-clés: syénite, feldspath, ré-équilibration post-magmatique, degré d'ordre Al-Si, perthite, rapport isotopique d'oxygène, hématite, Baie-des-Moutons, Québec, rift du St-Laurent.

INTRODUCTION

The Baie-des-Moutons ring complex, predominantly syenitic at the present level of erosion, is a rift-related pluton formed in the early Paleozoic along the northern boundary fault of the St. Lawrence graben (Higgins 1982). It is located 530 km ENE of Sept-Îles and 130 km W of the Labrador border, at La Tabatière, Québec (Fig. 1). The topographically prominent complex was first noted by Longley (1944) and later by Kranck (1961) and Hale (1962). Davies (1963, 1965a, b, 1968) described and mapped the ring complex in detail. His survey led to the definition of three major periods of cone-sheet emplacement; the validity of his *early*, *intermediate* and *late* groups has been confirmed during this project. Gold & Grencher (1967) and Grencher (1968) studied the geochemistry and paleomagnetism of dyke swarms associated with the complex. Our petrological investigation, which complements the previous studies, focuses on an evaluation of 1) the important intensive vari-

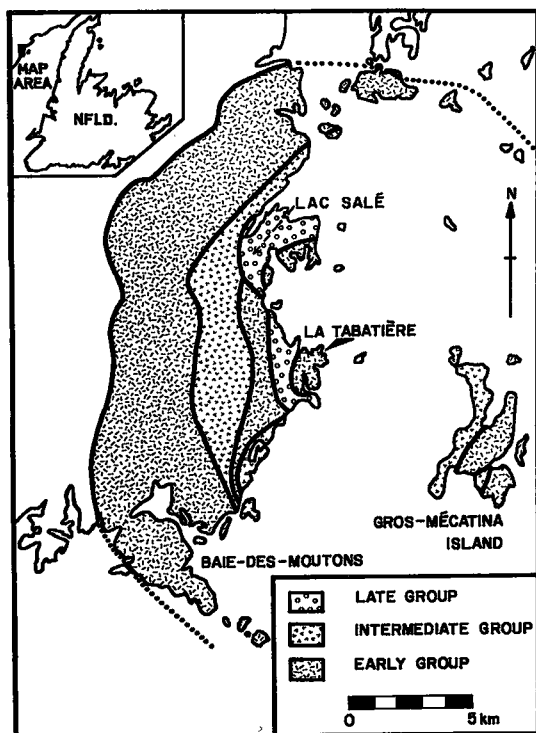


FIG. 1. Simplified geological map of the Baie-des-Moutons igneous complex, showing the distribution of the early, intermediate and late groups of cone-sheets. The map covers an area between lat. $50^{\circ}44'$ and $50^{\circ}57'$ N., long. $58^{\circ}50'$ and $59^{\circ}06'$ W.

ables during magmatism and 2) the degree of postmagmatic interaction with an aqueous fluid phase. In this report, we examine the texture, structural state, bulk composition and stable-isotope geochemistry of the feldspars, by far the dominant mineral group in all the rocks. In particular, we will explore the implications of the reddening of K-rich feldspars. A companion paper (Lalonde & Martin 1983) will illustrate the textures and mineral chemistry of the associated ferromagnesian minerals. However, we first discuss the general geology and petrography of the ring complex, because very little of this background information is readily available in print.

GEOLOGY OF THE RING COMPLEX

The complex, approximately 24 km in diameter, is dissected by the north shore of the Gulf of St. Lawrence; the numerous islands

provide ideal sites for sampling the internal cone-sheets (Fig. 1). The cone-sheets near the margins of the complex are nearly vertical, but those near the centre dip at a somewhat shallower angle. Davies (1968) recognized 23 map units among the coarse-grained alkali feldspar syenites, alkali feldspar quartz syenites, syenites and alkali feldspar granites (IUGS system of nomenclature). Although texturally mostly massive, some units (especially in the late group) have an igneous foliation that outlines the funnel-shaped structure of the intrusive complex. In the light of our field studies, the 23 units of Davies are grouped here and redefined as 13 distinct cone-sheets (see below) that constitute the early (units 1 \rightarrow 8), intermediate (units 9 \rightarrow 11) and late groups (units 12, 13).

The complex was emplaced in the early Cambrian [577, 562 Ma; ages by Rb-Sr geochronology on early and late groups, based on analyses of minerals reported by Doig & Barton (1968)] in Proterozoic gneisses of the Grenville structural province. These gneisses, largely granitic, pelitic and amphibolitic, are complexly folded and metamorphosed in the upper amphibolite to granulite facies (Bourne *et al.* 1978). The contact, well exposed in only two or three localities, consists of a 1-m-wide zone of feldspathization. No contact aureole or chilled margin is evident.

On aeromagnetic maps (5142 G, 5143 G, Aeromagnetic Series of the Department of Energy, Mines and Resources, published in 1969), the complex is outlined by a slightly higher-than-background intensity of the magnetic field, presumably a reflection of the importance of magnetite as an accessory phase in these syenites. The pattern of anomalies also outlines the contact with the host rocks and arcuate shape of some cone-sheets. The geometry of the intrusive body and the possible association of concealed mafic or anorthositic cumulates, facts that are important to know in petrogenetic discussions, could be provided by a detailed gravimetric survey. Unfortunately, the density of gravity stations over the complex is at present insufficient to elaborate on these topics.

PETROGRAPHY OF THE UNITS

Early group

The early group of syenitic cone-sheets, characterized by great thickness and lateral continuity (Fig. 1), makes up the periphery and centre of the pluton. The syenites are coarse

TABLE 1. SUMMARY OF MODAL ANALYSES OF SPECIMENS OF SYENITE FROM THE VARIOUS UNITS

UNIT	1	2	3,5	4	6	7	8	9	10	11	12	13
perthite	75-85	70-80	75-94	88-90	78	92	53-88	68-90	80-82	72-90	47-70	75-93
plagioclase	< 3	5-15					0-30*		0-3	0-7		
quartz	tr.	5	1-5	0-3	3		5	1-20		0-1		tr.
olivine											0-1	
orthopyroxene	tr.	tr.										
clinopyroxene	3-5		tr.	1-4				0-2		0-5	20	
amphibole	2-5	7			15	6	5-9	3-15	12-13	6-15	2-10	2-12
biotite	5-7		3-10	2-5	tr.	1	1-6	0-5	2-3	0-2	10	4-10
uralite			1-10	2-3	3							
iddingsite	< 1									0-2	< 1	
chlorite		tr.	tr.		tr.				tr.	0-2		tr.
serpentine										0-2	0-2	
calcite	tr.		tr.	tr.	tr.				< 1	0-2		tr.
opaque minerals	2-5	2	1-5	1	1	1	1	1-2	1-2	0-3	2-7	1-3
apatite	1-2	tr.	tr.	tr.	tr.	tr.	tr.	tr.	tr.	tr.	< 2	tr.
zircon		tr.	tr.	tr.	tr.	tr.	tr.	tr.	tr.	tr.	tr.	tr.
titanite			tr.	tr.		tr.	tr.					0-1
plagioclase composition	An ₁₂	An ₁₅							An ₅	An ₁₀		

* in xenocrystic cores

grained and generally massive. Each unit may contain pink and green variants. In all cases in the early group, the ferromagnesian minerals seem to have been liquidus phases. Eight distinct map-units [see Lalonde (1981) for a more detailed map of the units than is possible to show in Fig. 1; this map is available from the authors upon request] are listed here in a chronological sequence consistent with field observations: 1) coarse-grained green syenite, 2) coarse-grained green syenite to quartz syenite, 3) coarse-grained pink alkali feldspar syenite to quartz syenite, 4) coarse-grained foliated alkali feldspar syenite, 5) like 3, 6) medium- to coarse-grained green alkali feldspar syenite, 7) pinkish grey foliated alkali feldspar syenite, and 8) brownish pink, xenocryst-rich alkali feldspar syenite to quartz syenite. Representative modal compositions are reported in Table 1.

In the green pyroxene-bearing syenite of unit 1, centred near La Tabatière (Fig. 1), the mesoperthitic feldspar (~80 vol.%) displays a very coarse patchy perthitic intergrowth and commonly contains a xenocrystic core of oligoclase. Minute green and opaque specks are abundant in the perthite. Amphibole and biotite replace pyroxene preferentially along crystal margins, cleavages and fractures; the same late events that caused this replacement probably led to the development of ragged rims of biotite and titanite on the opaque minerals. Apatite and zircon are prominent accessory phases in clusters of ferromagnesian minerals. Locally, the rock may be greenish pink and biotite-bearing; this biotite clearly formed before the feldspars. The rock contains miarolitic cavities and pegmatitic pods, considered to be signs of

local water-saturation in the magma near the end stages of crystallization (Jahns & Burnham 1969).

Unit 2 occurs predominantly in the north-western corner of the intrusion, as a thin crescentic sheet near the contact with the gneissic host rocks. The presence of quartz and the overall similarity to rocks of unit 1 suggest that unit-2 syenites may have crystallized from a locally contaminated syenitic magma. Quartz clearly is interstitial; the opaque minerals in this unit poikilolithically enclose the other minerals, and from field evidence seem to have formed from a late-crystallizing (immiscible?) oxide-rich liquid (Lalonde & Martin 1983).

Units 3 and 5 form the most voluminous cone-sheets of the complex. These syenites are generally pink and commonly miarolitic. Feldspars attain 2 cm in length, and may be strongly color-zoned, from a green, iridescent, cryptoperthitic core to a pink mesoperthitic rim. The primary pyroxene crystals are strongly uralitized or replaced by biotite and chlorite. Hydrothermal effects are widespread in rocks of units 3 and 5.

In unit 4, a 1.6-km-thick sheet of pink syenite exposed near Baie-des-Moutons, the feldspar crystals are idiomorphic and may define a moderately well-developed foliation. Also found are the color zoning and the iridescence noted above: in some rocks, the pink rim, characterized by greater turbidity and a coarser perthitic texture than in the core, seems to have almost completely encroached on the green core. The mafic assemblages have undergone important postmagmatic changes, as noted above in connection with units 3 and 5.

In the syenite of unit 6, exposed in the northwestern part of the complex, the feldspar is mostly of the vein-perthite variety, but may contain a xenocrystic core of cryptoperthite or oligoclase. Primary-looking amphibole is dominant and may have arisen by a reaction relationship with the melt, as numerous small clusters of pyroxene are engulfed by amphibole.

Unit 7 is a 0.6-km-thick sheet of pinkish grey foliated syenite that intrudes unit 3. The feldspar, typically vein and braid perthite, lacks the cryptoperthite or oligoclase cores. Amphibole crystals seem primary and are relatively free of late transformations.

Syenites of unit 8, at the southwestern edge of the ring complex, contain abundant xenocrystic cores of plagioclase (composition An_{17-24}) in braid perthite grains and xenoliths of grey syenite. The main ferromagnesian mineral, hornblende, is interstitial here and typically retrograded to biotite; feldspars crystallized early, followed by ferromagnesian minerals. Quartz appeared very late in the sequence of crystallization.

Intermediate group

The following features characterize the syenites of the intermediate group: 1) they are predominantly grey-colored units; 2) their texture is intermediate between those of the early and late groups, *i.e.*, the syenites may be massive or well foliated; 3) they contain ferromagnesian minerals that typically crystallized *after* the feldspars, giving rise to strikingly poikilitic textures. These units occupy a transitional zone between the centre and periphery of the intrusion (Fig. 1).

Rocks of unit 9 occur in a continuous crescent-shaped cone-sheet up to 2 km thick ex-

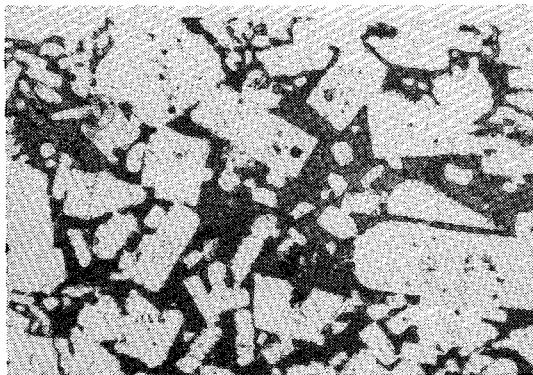


FIG. 2. Poikilitic amphibole enclosing numerous euhedral laths of perthite. Grey syenite, intermediate group. Plane light; field of view 3 mm.

tending southward from the Lac-Salé area (Fig. 1). Important internal textural and compositional variations are evident among the porphyritic olive grey syenites, quartz syenites and the greyish granites that make up this unit. The feldspar crystals commonly have a grey core and a pink rim. The ferromagnesian minerals form patches interstitial to the lath-shaped grains of feldspar. Quartz invariably is present, and locally may account for 20 vol.% of the rock. Amphibole, which predominates over pyroxene, contains irregular zones, rims and patches of blue-pleochroic domains. Biotite is minor and rims the amphibole and opaque minerals. Cryptoperthite xenocrysts commonly occur as cores in the phenocrysts; the interface between the two generations of perthite is decorated with abundant ferromagnesian inclusions. The cross-hatched pattern typical of microcline is obvious in the more quartz-rich specimens.

The feldspar phenocrysts in rocks of unit 10, exposed 3 km west of La Tabatière, are embedded in a matrix of feldspar and ferromagnesian minerals. Plagioclase xenocrysts occur as cores in perthite grains; their shape is outlined by abundant mafic inclusions. The interstitial amphibole shows transitions from green- to blue-pleochroic zones. Its alteration to calcite occurs along specific channelways in the rock. Quartz (minor) is associated with conspicuous clear rims of albite on the feldspar phenocrysts.

Unit 11 groups numerous thin cone-sheets of well-foliated greyish syenite found on Gros-Mécatina Island and southwest of La Tabatière (Fig. 1). Only the largest feldspar grains show dark cryptoperthitic cores. The anhedral ferromagnesian minerals (mainly amphibole) clearly are interstitial and strikingly poikilitic in habit (Fig. 2). Locally important alternations of planar felsic and mafic minerals may indicate movement and deformation while crystallization was still in progress. The pyroxene has a pleochroic scheme that suggests aegirine-augite, and the amphibole shows blue-pleochroic patches and rims. The opaque minerals and zircon also display the poikilitic textures.

Late group

Syenites of units 12 and 13 are coarse grained, very well foliated, and either green or pink. Igneous layering is defined by mafic segregations. The cone-sheets are generally thin and occupy the central portion of the complex (Fig. 1). Unit 12 is found in the Lac-Salé area; the dark green foliated syenites contain perthite laths 2 cm long. The mafic-mineral-rich layers may, on outcrop scale, define continuous

rhythmic banding, but textural evidence (*e.g.*, a subophitic texture) precludes a straightforward cumulate origin. Unaltered fayalitic olivine was found only in this unit, though its former presence is inferred in many others. The amphibole and biotite poikilitically enclose deep green pyroxene, zircon and the feldspars. The perthitic texture is distinctly coarser in the vicinity of biotite flakes.

Unit 13 is more widespread than unit 12; these orange pink foliated syenites occupy a 1-km-wide crescent around unit 1 (Fig. 1). The Carlsbad-twinning feldspar laths attain 2 cm in length, as do the interstitial amphibole crystals. This unit may have been emplaced as a crystal mush, as the mafic layers noted in the previous paragraph may be cross-laminated. Also, angular xenoliths of fine- to medium-grained equigranular to slightly porphyritic grey syenite are common. Pyroxene coexists with amphibole and voluminous opaque minerals in the melanocratic layers.

TEXTURES OF THE FELDSPARS

Early group

Feldspars from the coarse-grained green syenites of unit 1 consistently show interlocking perthite textures [Fig. 3; the nomenclature of Andersen (1928) is used here to describe the perthite]. The interlocking domains, from 0.02 to 0.4 mm across, consist of albite (typically albite-twinning) and K-feldspar that in turn, contains films of albite 0.04 mm thick. Minor cryptoperthitic (the term is used here without connotation of coherency between the two phases) areas occur, especially in the cores of the larger phenocrysts; also found in cores are plagioclase xenocrysts that exhibit zoning and possible resorption features. Minute inclusions of biotite, epidote and opaque minerals are peppered throughout the feldspar crystals of this unit; sericite and abundant apatite inclusions also are observed. The texture illustrated in Figure 3 is consistent with early exsolution of Na- and K-rich feldspars from an originally homogeneous magmatic K-feldspar (presumably sanidine), important recrystallization of the original cryptoperthitic intergrowth and continued exsolution in the K-rich domains at a lower temperature.

Perthitic feldspar from unit 6 (medium- to coarse-grained green alkali feldspar syenite) resembles that in unit 1 but displays a higher irregularity of intergrowth textures. Cryptoperthitic cores may be surrounded by patch, interlocking and vein perthites. Xenocrysts of plagioclase and perthite occur as cores in the

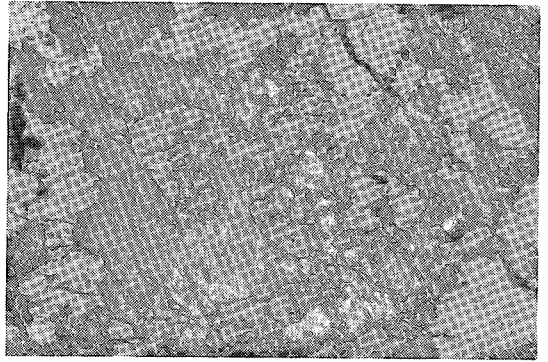


FIG. 3. Interlocking perthite from green syenite of the early group (unit 1). Note the presence of film albite in the K-rich domains. Crossed polars; field of view 3 mm.

perthite phenocrysts of this unit. Perthite xenocrysts contain prominent disseminated inclusions of opaque minerals, biotite, chlorite and apatite, all usually 0.02 to 0.1 mm across. Plagioclase xenocrysts, however, are devoid of such inclusions but display rims of fine opaque grains 0.002 to 0.1 mm across, larger flakes of biotite and possibly chlorite, and also fine apatite needles up to 0.04 mm in length. These plagioclase xenocrysts show zoning and albite twinning, and are commonly crossed by late, chlorite-filled fractures.

Feldspar grains from the pink alkali feldspar syenites to alkali feldspar quartz syenites (units 3 and 5) display very consistent differences in texture of the intergrowth between dark cores and coexisting pink rims. The greenish grey cores typically display blue iridescence in hand specimen, an optical diffraction effect caused by regularly spaced cryptoperthitic exsolution lamellae whose spacing is comparable to the wavelength of light (Smith 1974). The turbid reddish rims contain interlocking perthite with visible domains 0.04 to 0.4 mm across; minor patch and vein perthites also are observed. Sodic domains commonly achieve sufficient coarseness to permit the identification of albite twinning. The transition from cryptoperthitic cores to the turbid rims is gradational, as revealed by a coarsening of the scale of intergrowths and a dramatic increase in turbidity of the K-rich areas towards the rim of a grain (Figs. 4A, 4B). Also, the transformation to coarser turbid intergrowths is visibly more advanced along the numerous fractures that transect the cryptoperthitic cores (Fig. 4C); however, some thin fractures are outlined only by an increase in turbidity (*i.e.*, without coarsen-

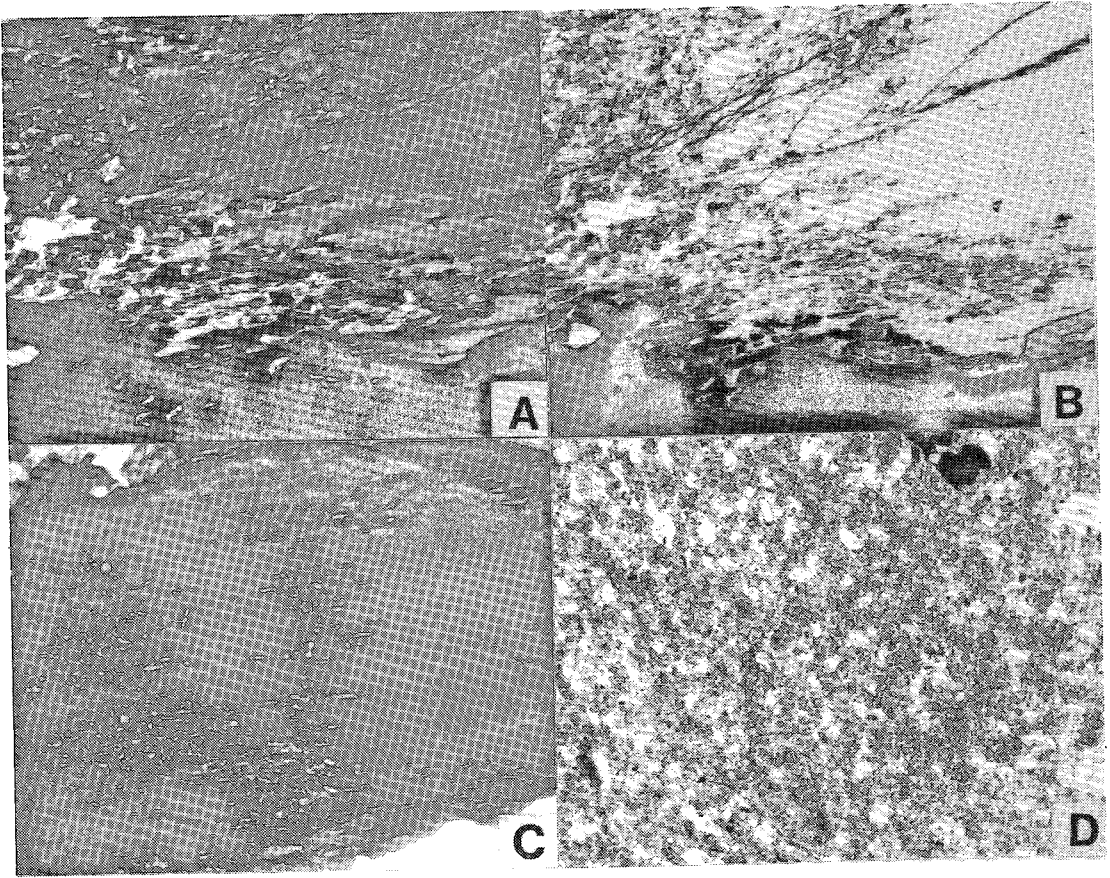


FIG. 4A. Coarsening of intergrowth textures from cryptoperthite in the core to interlocking perthite in the rim of the phenocryst. Unit 5. Crossed polars; field of view 3 mm. B. As in A, but in plane light. Note the increase of turbidity toward the rim of the phenocryst. C. Preferential transformation of cryptoperthite to coarser, turbid intergrowth along transecting fractures. Unit 3. Crossed polars; field of view 7.5 mm. D. Homogeneously distributed turbidity in K-rich domains of a single perthite grain from unit 4. Plane light; field of view 3 mm.

ing of intergrowth). Feldspar grains adjacent to miarolitic cavities are among the most turbid and coarsely intergrown of the unit; as in the rim-and-core situation, the intergrowth coarsens (to domains > 1 mm across) and the K-feldspar reddens toward the wall of the cavity. Cleavage traces appear as fine white lines in these highly turbid K-feldspars. Mineral inclusions are abundant, but by no means so prevalent as in the green perthite of units 1 and 6. Apart from acicular opaque minerals, the cryptoperthitic cores generally remain free of inclusions. In contrast, the turbid zones contain abundant inclusions of epidote, biotite and opaque minerals.

In unit 4, the coarse-grained, foliated, pink alkali feldspar syenites, the feldspar grains

typically are even more extensively affected by postmagmatic changes. They are characterized by intense and homogeneously distributed turbidity in the potassic domains (Fig. 4D). Intergrowths are principally of the interlocking type, with discrete domains 0.1 to 0.4 mm across. Cryptoperthitic cores are rarely seen. Sodic domains remain free of turbidity and commonly are albite-twinning. Microcline grid-twinning is evident only in grains adjacent to late quartz-calcite veinlets.

Feldspar grains from the pinkish grey foliated alkali feldspar syenites (unit 7) display well-formed braid- and vein-perthite. In this unit, potassic domains are invariably turbid and commonly display the grid twinning characteristic of microcline. Sodic lamellae are ≤ 0.04 mm

in thickness and only rarely exhibit albite twinning. Particularly well developed along perthite grain margins are late, nonturbid, sutured albite overgrowths up to 0.3 mm thick. The few mineral inclusions noted consist essentially of opaque minerals approximately 0.3 mm across.

Rocks of unit 8 (brownish pink xenocryst-rich alkali-feldspar quartz syenite) contain lamellar vein perthite with albite lamellae up to 0.3 mm thick. Slight branching of lamellae and localized coarsening to patch perthite occur. Plagioclase xenocrysts An_{17-24} in composition [combinations of Michel-Lévy, $Z \wedge (001)$ and $Y \wedge (010)$ methods] are particularly abundant in this unit. These xenocrysts are albite-twinning and invariably mantled by vein perthite. As suggested by thin exsolution lamellae, presumably K-rich, these xenocrystic cores were once ternary feldspar. They attain 2 cm across, but generally are < 0.5 cm, though conspicuous, owing to a white coloration on weathered surfaces. Inclusions of apatite, opaque minerals, epidote, titanite and, especially, biotite can account for as much as 20% by volume of the xenocrysts. Grain margins of clear albite \leq 0.02 mm thick are common and are associated with late quartz. The cross-hatched pattern typical of microcline is not widespread.

Intermediate group

Despite the great petrographic variability of the undifferentiated grey alkali feldspar syenites to alkali feldspar granites (unit 9), perthitic intergrowths encountered are, with few exceptions, vein perthites. In these grains of feldspar, albite occurs as veinlets 0.02 to 0.1 mm thick, rarely albite-twinning, coexisting with moderately turbid potassic domains. These commonly show the characteristic cross-hatched pattern of well-ordered microcline. Also observed as intergrowth textures within this unit are branching vein- and braid-perthite. Cryptoperthite does occur, mainly as xenocrystic cores rich in inclusions, mantled by vein perthites. Late albite forms a clear rim around perthite grains.

In unit 10, the porphyritic grey alkali feldspar syenite, the main intergrowth texture encountered is patch perthite, with vein perthite second and braid perthite a distant third in abundance. Average diameters of potassic domains in the patch perthite range from 0.15 to 0.6 mm. Potassic and sodic domains show microcline grid-twinning and albite twinning, respectively. Cleavage traces generally appear as thin white lines in the highly turbid potassic domains. Large perthite phenocrysts from this porphyritic unit invariably have antiperthitic xeno-

crystic plagioclase cores; zoning in the core is evident from the variable extinction angles. In view of the fine K-rich lamellae, these antiperthitic plagioclase xenocrysts appear to have been ternary feldspar. Inclusions of biotite, carbonates and opaque minerals are numerous. Sutured rims of late albite form around perthite phenocrysts.

Few generalizations can be made concerning perthite textures in the foliated grey alkali feldspar syenite of unit 11. Patch, vein and braid perthites are the most common, but other types also are encountered. The extent of coarsening of these intergrowths also is variable, and cryptoperthitic cores are common; K-feldspar, especially in braided intergrowths, commonly displays microcline grid-twinning; albite twinning of sodic domains also is common. A perthite xenocryst commonly forms the core of larger perthite phenocrysts in this unit.

Late group

These syenites are distinguished by their euhedral, lath-shaped perthite phenocrysts and by the excellent trachytic texture that the phenocrysts define. In the green syenites (unit 12), the phenocrysts are essentially cryptoperthitic, though some coarsening to braid or patch perthite occurs. In the braid perthites, lozenge-shaped K-rich domains seldom exceed 0.1 mm before a patch-perthite pattern becomes dominant. The coarsening of intergrowth textures, accompanied by the usual increase in turbidity, does not appear to follow any specific path or pattern of distribution with respect to phenocrysts or matrix. In the orange pink analogues (unit 13), the coarsening of intergrowth textures and the development of turbidity have obviously progressed further. Cryptoperthite remains abundant, but many feldspar grains display either patchy or interlocking textures. In most cases, coarsely intergrown turbid zones occupy the margins of phenocrysts. Yet, this distribution is not as pronounced as in examples from the early group. As is evident from the orange pink (locally brownish) color of feldspars, the extent of turbidity is generally not as great as in the pink syenites of the early group. In the coarser intergrowths, albite twinning is commonly visible in sodic domains; microcline grid-twinning, expected only in well-ordered microcline, was not observed.

STRUCTURAL STATE AND COMPOSITION OF THE FELDSPARS

Cell refinements were performed on both the K- and Na-rich phases of 23 perthite grains

TABLE 2. SUMMARY LISTING OF CELL PARAMETERS FOR COEXISTING FELDSPARS FROM THE EARLY, INTERMEDIATE AND LATE GROUPS

Sample	a	b	c	α	β	γ	V	α^*	β^*	γ^*	$\Delta 2\theta$	N_{0r}	$\Delta(bc)\Delta(\alpha^*\gamma^*)$	t_{10}	t_{1m}	t_{20}	
P8650	8.5653	12.9893	7.1939	90	115.995	90	719.40	90	64.004	90	.008	0.899	0.745	0	0.372	0.372	0.128
EG	0.0010	0.0016	0.0007		0.008		0.10		0.008		20						
	8.1485	12.8233	7.1402	94.007	116.510	86.608	665.91	86.217	63.521	89.557	.010	0.004	0.787	0.636	0.712	0.075	0.106
	0.0010	0.0015	0.0007	0.013	0.012	0.012	0.11	0.013	0.012	0.012	24						
77-1228	8.5765	12.9693	7.2123	90.360	115.983	88.263	720.79	90.445	64.015	91.757	.009	0.937	0.920	0.748	0.834	0.086	0.040
EG	0.0015	0.0016	0.0008	0.013	0.012	0.013	0.11	0.012	0.011	0.012	24						
	8.1354	12.7824	7.1591	94.272	116.598	87.623	663.80	86.412	63.495	90.522	.009	-0.023	0.992	1.018	1.005	0.013	0.004
	0.0007	0.0012	0.0009	0.008	0.008	0.008	0.09	0.010	0.009	0.008	34						
78-25A	8.5919	12.9934	7.1985	90	116.092	90	721.73	90	63.909	90	.015	0.965	0.766	0	0.383	0.383	0.117
rim	0.0017	0.0017	0.0015		0.015		0.16		0.015		21						
	8.1406	12.7817	7.1661	94.278	116.700	87.935	664.27	86.248	63.374	90.162	.006	-0.017	1.037	0.893	0.965	0.072	0.018
	0.0008	0.0008	0.0004	0.007	0.007	0.008	0.08	0.007	0.006	0.010	23						
78-25A	8.6001	12.9622	7.1932	90	116.095	90	720.19	90	63.906	90	.011	0.921	0.806	0	0.403	0.403	0.097
core	0.0011	0.0020	0.0008		0.010		0.13		0.010		29						
	8.1331	12.8122	7.1582	94.252	116.607	87.900	665.06	86.295	63.469	90.220	.015	-0.008	0.922	0.909	0.916	0.006	0.039
	0.0014	0.0021	0.0014	0.032	0.020	0.025	0.18	0.032	0.019	0.027	22						
P8655	8.5850	12.9610	7.2155	90.642	115.960	87.828	721.32	90.345	64.044	92.103	.010	0.953	0.962	0.938	0.950	0.012	0.019
IG	0.0011	0.0022	0.0007	0.015	0.010	0.013	0.12	0.013	0.010	0.012	28						
	8.1398	12.7931	7.1620	94.223	116.650	87.710	664.74	86.423	63.438	90.445	.009	-0.011	0.987	0.982	0.985	0.002	0.007
	0.0006	0.0010	0.0007	0.008	0.007	0.008	0.07	0.007	0.007	0.007	35						
77-2285	8.5752	12.9754	7.2099	90.465	115.963	88.395	720.97	90.265	64.039	91.558	.010	0.942	0.889	0.693	0.791	0.098	0.056
LG	0.0010	0.0013	0.0010	0.010	0.012	0.013	0.10	0.010	0.012	0.012	22						
	8.1449	12.7833	7.1584	94.268	116.622	87.720	664.45	86.368	63.467	90.413	.008	-0.015	0.985	0.979	0.982	0.003	0.007
	0.0007	0.0014	0.0005	0.008	0.007	0.008	0.08	0.008	0.006	0.010	24						
78-40	8.5855	12.9758	7.1968	90	116.060	90	720.24	90	63.939	90	.015	0.922	0.798	0	0.399	0.399	0.101
LG	0.0024	0.0027	0.0026		0.025		0.28		0.025		15						
	8.1389	12.7914	7.1524	94.217	116.625	87.886	663.85	86.342	63.451	90.252	.011	-0.022	0.931	0.914	0.923	0.009	0.034
	0.0008	0.0015	0.0009	0.010	0.010	0.012	0.10	0.010	0.010	0.012	24						

Abbreviations: EG early group, IG intermediate group, LG late group. Units: a , b , c in Å, unit-cell volume V in Å³, α , β , γ , α^* , β^* , γ^* , $\Delta 2\theta$ (standard error) in degrees. N_{0r} is expressed in mole fraction. The values $\Delta(bc)$ and $\Delta(\alpha^*\gamma^*)$, which are equivalent to $t_{10}+t_{1m}$ and $t_{10}-t_{1m}$, respectively, were calculated using the program of Blasi (1977); t_{10} represents the Al occupancy of the T_{10} position in the feldspar. In each case, the K-feldspar data are listed first; the third and fourth lines contain the data for the coexisting sodic feldspar in the perthite. # number of indexed peaks used.

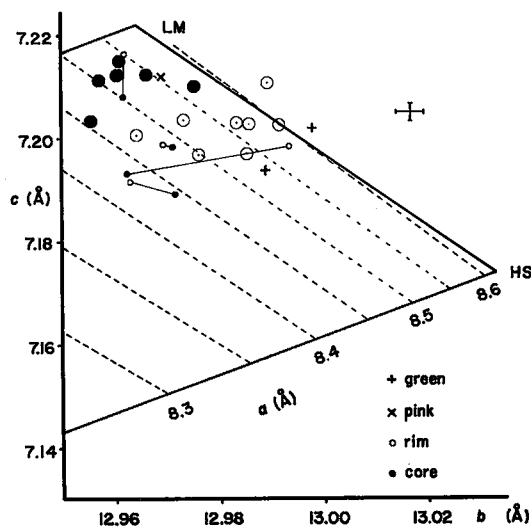


FIG. 5. Plot of b versus c for feldspars in pink, green and color-zoned perthite grains in syenite from the early group. Phenocryst rim and core values are linked by a tie line. The K-feldspar from the intermediate group (generally microcline, ●) and from the late group (generally orthoclase, ○) are also shown. Error bars represent the average standard error in b and c .

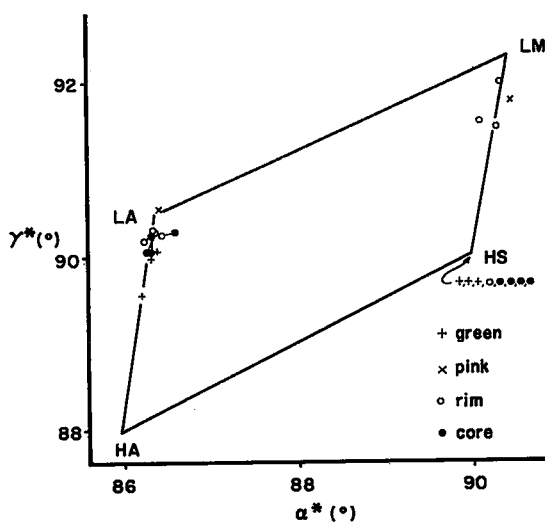


FIG. 6. Plot of α^* versus γ^* for feldspars in pink, green and color-zoned perthite grains in syenite from the early group. Values of sodic feldspars from phenocryst rim and core are joined by a tie line. This was not done for the K-rich feldspar data-points for the sake of clarity; tie lines all radiate from the HS corner. The dimensions of the symbols in this diagram exceed the average errors.

from specimens of the three groups. Indexed and corrected 2θ reflections served as input to the program of Appleman & Evans (1973). Patterns were acquired with a Guinier-Hägg focusing camera ($\text{CuK}\alpha_1$ radiation). The correction procedure involved a comparison of predicted and observed positions of diffraction maxima of a synthetic MgAl_2O_4 internal standard (a 8.0833 Å at room temperature; G.V. Gibbs, pers. comm.). Errors associated with the refined cell-edge dimensions were seldom found to exceed 2×10^{-3} Å. Representative results for green, grey and pink feldspars from the early, intermediate and late groups are shown in Table 2. A complete listing of all the cell parameters is available in Lalonde (1981).

Early group

The striking differences in feldspar color, from greenish grey to pink, coincide with a major difference in feldspar mineralogy: both sodic and potassic feldspars in perthite grains of the pink syenites approach ordered states more closely than those in the green syenites. Both the b - c and α^* - γ^* plots (Figs. 5 and 6, respectively) illustrate that the K-feldspar from specimens of green syenite generally is monoclinic to X rays (*i.e.*, orthoclase), whereas in specimens of pink syenite, intermediate microcline ($t_10 \sim 0.83$) is encountered. Furthermore, albite from green syenite is *apparently* more disordered than in the pink units. However, this departure from the low albite corner in Figure 6 largely reflects the presence of calcium in the structure (see below).

X-ray-diffraction patterns of perthite grains from units 3 and 5 confirm the systematic differences in feldspar mineralogy between the turbid pink rims and the dark grey or green cores. On the α^* - γ^* plot (Fig. 6), sodic feldspar in the rim apparently is better ordered than its counterpart from the core. Also, K-feldspar in the core generally is monoclinic to X rays: the adjacent rim contains, in general, a more evolved feldspar, either orthoclase that is less strained, or intermediate microcline (Fig. 5).

The differences in feldspar mineralogy between rim and core suggest that low-temperature re-equilibration has progressed further in the rim. This interpretation is supported by the persistence of the most intense peaks of orthoclase (*e.g.*, 201, 130, 220, 002) in the diffraction pattern of microcline from turbid zones. The diffraction maxima of orthoclase from the core are broad, consistent with incipient breakdown to a tricline cell. Traces of the dominant

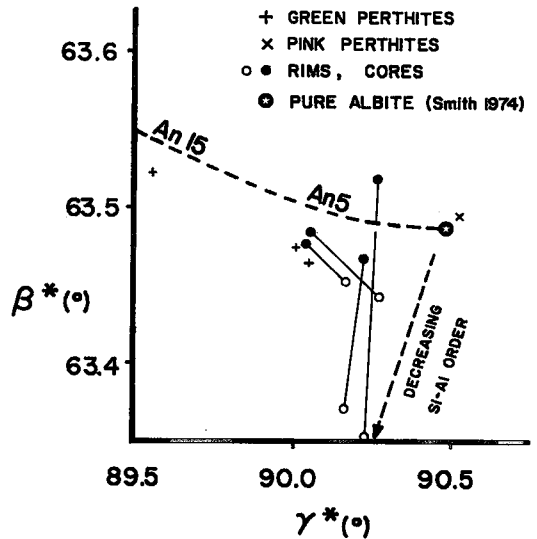


FIG. 7. Plot of β^* versus γ^* for the sodic plagioclase from the pink, green and color-zoned perthite grains in syenite from the early group. Phenocryst rim and core values are linked by a tie line. The dimensions of the symbols exceed the average errors.

reflections of intermediate microcline are also commonly encountered in powder pattern of core-zone orthoclase.

The departure of data points from the low albite corner in the α^* - γ^* plot (Fig. 6) reflects mainly compositional (rather than structural) effects. To evaluate An content, the β^* - γ^* plot of Smith (1974) can be used. On the basis of this plot (Fig. 7), green syenites contain "ordered" calcic albite to oligoclase (up to An_{10}). Albite in the core of a color-zoned grain is more calcic than in the adjacent rim (joined by a tie line in Fig. 7). Note that the rim albite appears slightly disordered, plotting along a dashed line that represents the An_{10} isopleth in the direction of increasing Si-Al disorder.

Systematic differences in apparent lattice strain also are observed between coexisting greyish or greenish cores and pink rims of perthite phenocrysts. Strain in feldspars generally results from coherence between sodic and potassic phases in cryptoperthitic intergrowths (Yund 1975). Strain usually is measured according to the Δa index [$= a$ observed - a inferred from the b - c plot; Stewart & Wright (1974)]; a K-feldspar sample that has a Δa value in excess of 0.05 Å is considered strained. The a^* versus $Or(b^* c^*)$ plot of Blasi (1977; see also Blasi *et al.* 1980) provides another method of evaluating strain. On this diagram,

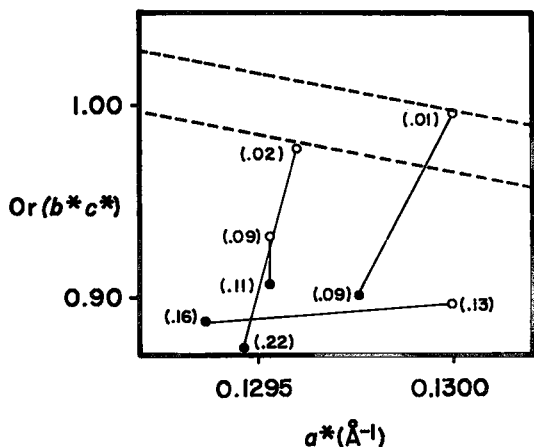


FIG. 8. Plot of a^* versus $Or(b^*c^*)$ for K-feldspar from coexisting rim of phenocryst (open circle) and core (solid circle) in pink syenite of the early group. Values of Δa (in Å) are shown in parentheses.

by convention, a band of ± 0.15 Or encloses unstrained K-feldspar (Smith 1974, Fig. 7-29) in the pink syenites of the early group. K-feldspar samples from contiguous rim and core are plotted on this diagram along with their respective Δa index (Fig. 8).

All specimens of rim K-feldspar plot above their respective core equivalents in $a^*-Or(b^*c^*)$ space. Furthermore, all rim K-feldspar has a smaller Δa value than its core counterpart. The variations in strain observed between coexisting rim and core K-feldspars are interpreted as a consequence of the difference in scale of exsolution between these respective domains. Core

cryptoperthites evidently comprise highly strained coherent intergrowths. Coarsening of exsolution domains in the phenocryst rims leads to a loss in coherency and removal of part of the lattice strain during the nucleation and growth of the more ordered feldspars.

Intermediate group

X-ray-diffraction patterns and cell parameters were obtained for 7 perthite specimens of the intermediate group. On a b versus c diagram (Fig. 5) as well as on a site-occupancy plot (Fig. 9), nearly all data points for K-feldspar show high t_{10} values and, thus, approach low microcline (2 out of 7 are orthoclase). Correspondingly, sodic feldspars from this group display high t_{10} occupancies (Table 2), probably a reflection of very low present (and original) calcium contents.

Late group

For the late group, unit-cell parameters were obtained for three grains of perthite from the orange pink syenites and one of the green syenites. As seen in Figures 5 and 9, the observed lack of highly turbid and extensively coarsened intergrowths correlates well with only limited Al-Si ordering of the K-feldspar. The green syenites of the late group contain the most disordered K-feldspar in this collection ($t_{10} = 0.40$); in addition, only one out of three specimens from the orange pink syenites (unit 13) is triclinic. Albite samples from the green unit have considerably higher calculated t_{10} occupancies than their counterparts from the early group and probably reflect, as in the intermediate group, lower original calcium contents (Table 2).

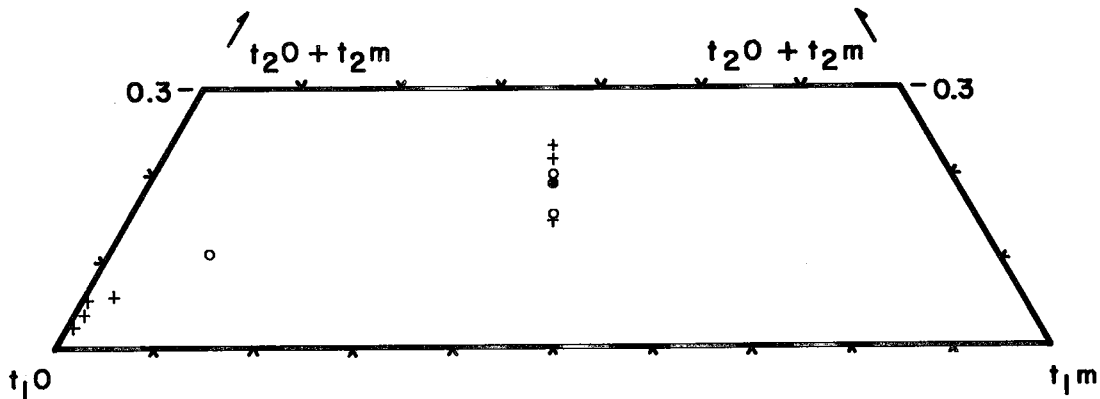


FIG. 9. Triangular site-occupancy plot of K-feldspar in grey perthite from the intermediate group (cross) and in orange pink (open circle) and green perthite (solid circle) from the late group.

ELECTRON-MICROPROBE DATA

Few reliable data could be obtained using the electron-microprobe technique. In addition to instrumental problems, the fine scale of the intergrowth led to aberrant intermediate compositions, because the electron beam sampled more than one compositional domain. The data do give semiquantitative evidence of plagioclase compositions in the range $An_{20} - An_{30}$ in the core zone. The first feldspar to form in these units evidently crystallized from liquids evolving in the system $Ab-An-Or$. The prominence of sodic andesine and oligoclase as xenocrystic cores in the green syenite of the early group suggests crystallization from less evolved liquids and at higher temperatures than their younger, xenocryst-free counterparts in the early group. The very low An content determined for sodic plagioclase in pink syenite of the early group is consistent with crystallization from a more evolved, lower-temperature liquid. Note that the albite and K-feldspar from pink rocks were also flushed of part of their Ca and Na , respectively, during postmagmatic recrystallization processes.

OXYGEN-ISOTOPE GEOCHEMISTRY

To characterize the source of the water involved in these transformations, oxygen-isotope determinations were performed on samples of feldspar picked from wholly pink and wholly green syenites, coexisting grey core and turbid rim from pink syenites, and from a late trachytic dyke composed essentially of extremely turbid, brick red alkali feldspar. Results (Yuch-Ning Shieh, pers. comm. 1979) presented in Table 3 show $\delta^{18}O$ values (relative to Standard Mean Ocean Water) in the range typical of fresh, mantle-derived igneous suites ($\delta^{18}O$ 5.5 to 7.0‰ for basalt, gabbro, syenite and andesite: Taylor 1968). Core and rim specimens from the same phenocryst yield identical ratios. From these data, we may conclude that water present during feldspar transformations was of magmatic origin, and thus locally derived. The miarolitic cavities in the pink syenite and the pegmatitic pods found in green syenite (unit 1) are evidence of local water-saturation at the end stages of magmatic crystallization (Jahns & Burnham 1969). Large-scale convection of meteoric water introduced through the host rocks surrounding the cooling pluton, as documented by Taylor & Forester (1979) for the upper part of the Skaergaard complex in eastern Greenland, can be ruled out. At Baie-des-Moutons, as in the lower part of the Skaergaard complex, the

TABLE 3. OXYGEN-ISOTOPE RATIOS OF SELECTED FELDSPAR SPECIMENS

Specimen	Intrusive unit	Description	$\delta^{18}O$ per mil
78-63	1	Green feldspar	7.1
78-87	4	Pink feldspar	6.6
78-79A2	5	Grey feldspar from phenocryst core	7.2
78-79A2	5	Pink feldspar from phenocryst rim	7.2
78-20B	*	Extremely turbid red feldspar	6.6

* Late dyke of red trachytic syenite. Analyses performed by Yuch-Ning Shieh (Purdue University).

country-rock gneisses undoubtedly are too impermeable to allow appreciable inflow of meteoric water. Furthermore, the presence of sharp boundaries between the green and pink units in both early and late groups precludes such a pervasive introduction of meteoric water at a subsolidus stage.

THE NATURE OF TURBIDITY: SEM EVIDENCE

The common red color of turbid alkali feldspar was originally ascribed to exsolution of iron from the crystal structure (MacGregor 1931), or even to incipient breakdown to kaolinite minerals. However, Folk (1955) pointed out the importance of fluid inclusions in causing the familiar cloudiness of these minerals. His findings were later confirmed by Boone (1969) in an investigation of reddened albite in granite from Gaspé, Québec. Boone found that cloudy red feldspar formed in the granite porphyry only if mafic silicates or oxides are simultaneously undergoing oxidation. To test the hypotheses of Folk and Boone, a perthite specimen from the early group, consisting of a translucent cryptoperthite core and coarsely intergrown turbid rim, was examined by scanning electron microscopy (Fig. 10A, B; see also Figs. 4A, B). There is clearly a much greater abundance of vacuoles in the rims than in cores. A detailed fluid-inclusion study (J. Guha, pers. comm., 1979) failed to demonstrate the presence of an aqueous fluid within these small ($\leq 0.5 \mu m$) vacuoles. We ascribe this "leakage" of the fluid phase to the well-developed system of cleavages and fissures in the recrystallized feldspar grains. We contend that the vacuoles reflect an overall decrease in volume as a result of (1) anisotropic thermal contraction, (2) exsolution, (3) nucleation of strain-free potassic domains, (4) increase in the degree of $Al-Si$ order and (5) net removal of some material by dissolution (Martin & Lalonde 1979) owing to the relatively high solubility of feldspar minerals in high-temperature aqueous phases (Burnham 1967, Currie 1968). The flaky mineral

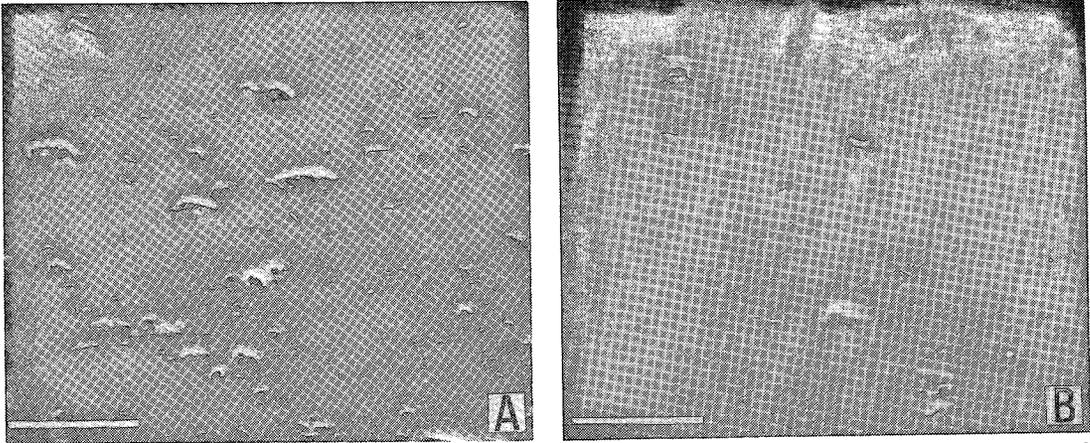


FIG. 10A. Surface texture of perthite from the rim of a color-zoned phenocryst. Note the abundance of small vacuoles. The surface was not etched. Scanning electron micrograph. B. Surface texture of the corresponding core zone. Note the lack of vacuoles. Parallel streaks are polish marks. Scanning electron micrograph; unit 5. Scale bar represents 20 μm in both cases.

that lines the vacuole walls yields intense peaks of iron on the electron microprobe, and is here interpreted to be hematite. This hematite, responsible for the striking pink coloration of the turbid feldspars in the rims, can be used as an indicator of postmagmatic dissolution of nearby ferromagnesian minerals under oxidizing conditions, as suggested by Boone (1969). Lalonde & Martin (1983) document more fully the intrinsic $f(\text{O}_2)$ of the magmas that crystallized to give the green and pink syenites.

DISCUSSION

Cryptoperthite is commonly accepted as the product of coherent exsolution, initiated by spinodal decomposition upon cooling and intersection with the coherent solvus (Yund & McCallister 1970, Yund 1974). Further coarsening of a perthitic intergrowth and consequent loss of coherency generally require the presence of a catalyst (Parsons 1978, 1980). In the case of perthite from Baie-des-Moutons, the selective coarsening of intergrowths from the rim inward and along fractures strongly suggests the presence of a mobile aqueous phase as the required catalyst. The abundance of hydrous minerals in the coarsened zones confirms H_2O as the main volatile component. The rate of Al-Si ordering in alkali feldspars is known to be a complex function of temperature, time, cooling rate and surface area. In addition, the presence of an aqueous fluid (Martin 1974) is critical in achieving an ordered configuration in the feldspars. Closely related to coarsening

of intergrowth textures and framework ordering is the development of turbidity, especially in the K-rich domains.

Within the pink syenite of the early group, an interstitial aqueous fluid evidently induced postmagmatic recrystallization of the perthitic feldspar, resulting in (1) coarsened, noncoherent domains, (2) increased Al-Si order in both sodic and potassic phases, (3) the appearance of minor amounts of hydrous minerals, including epidote to accommodate the Ca liberated by the plagioclase, (4) myriads of fluid inclusions lined with hematite. The actual mechanism by which these transformations occur probably involves numerous, very local solution-and-redeposition steps in a fluid progressing along margins and fractures toward the crystal's core (O'Neil & Taylor 1967). This mechanism may proceed to recrystallize the feldspar grain completely, leaving a homogeneously coarse and turbid intergrowth with few remaining relics of cryptoperthite (*e.g.*, unit 4, Fig. 4D).

Perthite from the green syenites of the early group also reacted with water, as manifested by the presence of a coarse interlocking intergrowth and numerous inclusions of hydrous minerals. However, the interaction could well have occurred (1) at higher temperatures (*e.g.*, $> 500^\circ\text{C}$), above the field of stability of microcline, and (2) at lower oxygen fugacities, not allowing free hematite to precipitate within vacuoles. The greenish coloration may be due to a hydrous, Fe^{2+} -bearing pigment (Orliac 1957), presumably liberated from the mafic phases during the early stages of interaction of the

completely disordered magmatic feldspar with the films and pockets of supercritical H_2O released at the end stages of crystallization.

Feldspar grains from the grey syenites of the intermediate group contain among the best ordered albite and microcline of the complex. This feature and their moderately turbid character but grey color constitute the salient characteristics of the feldspars in this group. Magmas that gave rise to these units of syenite were liquids (or crystal mushes in the foliated examples) emplaced exclusively in the thick cone-sheets of the early group. At this time, rocks of the early group, although sufficiently cooled to fracture, must still have been in the process of cooling. The cooling rate of the relatively thin cone-sheets of the intermediate group must have been highly influenced by the high output of heat from the much more voluminous host-rocks of the early group. As a result, a long, slow cooling period is believed responsible, in large part, for the almost perfect Al-Si order of intermediate-group feldspars. The preservation of primary crystal outlines, along with only a moderate development of turbidity, suggest that postmagmatic recrystallization of these feldspars in the presence of an aqueous fluid was efficient, yet possibly involved a lower proportion of water than in the early group. The mildly alkaline affinities in bulk-rock and mineral chemistry (Lalonde & Martin 1983) and the abundance of a late, pure albite decoration along perthite grain-margins suggest the presence of a peralkaline fluid, shown by Martin (1969) to furnish the most favorable environment for efficient Al-Si ordering.

Feldspars from the late group are characterized by a similar coloration scheme as in the early group. However, feldspars in the orange pink units are less turbid, have higher proportions of cryptoperthite, and are less ordered than their counterparts of the early group. This poor development of turbidity results in an orange pink to brownish color rather than true pink as in the early group. Also, these turbid feldspars generally have orthoclase as their potassic phase rather than intermediate microcline. These observations suggest restricted feldspar-water interaction in the orange pink units, probably at relatively high temperatures, mostly within the stability field of orthoclase or, possibly, during a shorter time period at temperatures below this field.

Green-colored syenites of the late group, unlike early-group analogues, show little or no coarsening of the perthitic intergrowths. Thus, in spite of limited interaction with water,

probably at low $f(O_2)$ as is evident from the lack of a red color or turbidity, these feldspars remained almost entirely in their pristine state. Sodic albite compositions in both pink and green units probably reflect the calcium depletion expected with increasing magmatic fractionation in the reservoir below (Parsons 1978).

The late group was emplaced as very thin cone-sheets within units of the early group at the centre of the complex. Potassium-argon ages performed on biotite from early and late groups (Davies 1968) yield a time lapse of 12 Ma. The thick early-group units had probably cooled completely during this interval. Unlike the case of the cone-sheets of the intermediate group, heat loss from the late cone-sheets thus was rapid; this would account for the observed mineralogical trends. However, why the latest units of the complex fail to show the expected buildup in water and other volatiles remains unknown.

The feldspars in the Baie-des-Moutons syenites illustrate well the disequilibrium assemblages typically encountered in an epizonal plutonic complex that cooled rapidly. Rocks of the intermediate group demonstrate the importance of considering the alkalinity of the bulk compositions and, inevitably, of the fluid medium, in understanding the more successful conversion of the magmatic feldspars to stable low-temperature assemblages. In the early and late groups, at least in rim assemblages and in pinkish units, the feldspars attained compositional equilibrium, but structural equilibration was not achieved.

ACKNOWLEDGEMENTS

Professors J. Guha (Université du Québec à Chicoutimi) and Yuch-Ning Shieh (Purdue University) provided fluid-inclusion and oxygen-isotope data, respectively. We gratefully acknowledge their contribution to this project. We thank Ann and Tom Robertson of La Tabatière for their hospitality during our visits to the field area. André Lalonde was introduced to the complex by Professor J. Bourne. Research expenses were covered by a Natural Sciences and Engineering Research Council grant (A7721) to R.F. Martin. Two referees selected by Associate Editor L.T. Trembath provided many helpful comments.

REFERENCES

- ANDERSEN, O. (1928): The genesis of some types of feldspar from granitic pegmatites. *Norsk Geol. Tidsskr.* 10, 116-207.

- APPLEMAN, D.E. & EVANS, H.T., JR. (1973): Job 9214: indexing and least-squares refinement of powder diffraction data. *U.S. Geol. Surv. Comp. Contr.* 20.
- BLASI, A. (1977): Calculation of T-site occupancies in alkali feldspar from refined lattice constants. *Mineral. Mag.* 41, 525-526.
- , BRAJKOVIC, A., BLASI DE POL, C., FORCELLA, F. & MARTIN, R.F. (1980): Contrasting feldspar mineralogy, textures and composition of Tertiary anorogenic and orogenic granites, Gilgit area, northwestern Pakistan. *Neues Jahrb. Mineral. Abh.* 140, 1-16.
- BOONE, G.M. (1969): Origin of clouded red feldspars: petrologic contrasts in a granitic porphyry intrusion. *Amer. J. Sci.* 267, 633-668.
- BOURNE, J.H., ASHTON, K.E., GOULET, N., HELMSTAEDT, H., LALONDE, A. & NEWMAN, P. (1978): Portions of the Natashquan, Musquaro and Harrington Harbour map-areas, eastern Grenville province, Quebec—a preliminary report. *Geol. Surv. Can. Pap.* 78-1A, 413-418.
- BURNHAM, C.W. (1967): Hydrothermal fluids at the magmatic stage. In *Geochemistry of Hydrothermal Ore Deposits* (H.L. Barnes, ed.). Holt, Rinehart and Winston, New York.
- CURRIE, K.L. (1968): On the solubility of albite in supercritical water in the range 400 to 600°C and 750 to 3500 bars. *Amer. J. Sci.* 266, 321-341.
- DAVIES, R. (1963): Geology of the St. Augustin area, Duplessis County, Quebec. *Que. Dep. Nat. Res. Prelim. Rep.* 506.
- (1965a): Geology of the Cook—d'Audhebourg area, Duplessis County, Quebec. *Que. Dep. Nat. Res. Prelim. Rep.* 537.
- (1965a) Geology of the Baie-des-Moutons area. Duplessis County, Quebec. *Que. Dep. Nat. Res. Prelim. Rep.* 543.
- (1968): *Geology of the Mutton Bay Intrusion and Surrounding Areas, North Shore, Gulf of St. Lawrence, Quebec*. Ph.D. thesis, McGill Univ., Montreal, Que.
- DOIG, R. & BARTON, J.M., JR. (1968): Ages of carbonatites and other alkaline rocks in Quebec. *Can. J. Earth Sci.* 5, 1401-1407.
- FOLK, R.L. (1955): Note on the significance of "turbid" feldspars. *Amer. Mineral.* 40, 356-357.
- GERENCHER, J.J. (1968): *Structural Relationships, Petrography, Chemistry, and Magnetic Properties of some Dike Swarms in and around the Mutton Bay Pluton, Quebec*. M.S. thesis, Pennsylvania State Univ., University Park, Pa.
- GOLD, D.P. & GERENCHER, J.J. (1967): Report on the Mutton Bay structure. In *Study of Structural and Mineralogical Significance of Meteorite Impact Sites, Including Mineral Paragenesis, High Pressure Polymorphs, Micro-fractures and Quartz Lamellae*. *Nat. Aeronaut. Space Admin. 4th Ann. Rep. (7th semi-annual rep.)*, 15-27.
- HALE, W.E. (1962): Geological reconnaissance, St. Augustin area, North Shore, Gulf of St. Lawrence. *Can. Mining Metall. Bull.* 55, 326-331.
- HIGGINS, M.D. (1982): Magmatism in the Grenville Province since the Grenville orogeny. *Geosci. Can.* 9, 118-121.
- JAHNS, R.H. & BURNHAM, C.W. (1969): Experimental studies of pegmatite genesis. I. A model for the derivation and crystallization of granitic pegmatites. *Econ. Geol.* 64, 843-864.
- KRANCK, E.H. (1961): The tectonic position of anorthosites of eastern Canada. *Comm. géol. Finlande Bull.* 196, 299-320.
- LALONDE, A.E. (1981): *The Baie-des-Moutons Syenitic Complex, La Tabatière, Québec*. M.Sc. thesis, McGill Univ., Montréal, Qué.
- & MARTIN, R.F. (1983): The Baie-des-Moutons syenitic complex, La Tabatière, Québec. II. The ferromagnesian minerals. *Can. Mineral.* 21, 81-91.
- LONGLEY, W.W. (1944): Aguanish River to Lobster Bay, North Shore of the Gulf of St. Lawrence. *Que. Dep. Mines Internal Rep. (unpubl.)*.
- MACGREGOR, A.G. (1931): Clouded feldspars and thermal metamorphism. *Mineral. Mag.* 22, 524-538.
- MARTIN, R.F. (1969): The hydrothermal synthesis of low albite. *Contr. Mineral. Petrology* 23, 323-339.
- (1974): Controls of ordering and subsolidus phase relations in the alkali feldspars. In *The Feldspars* (W.S. MacKenzie & J. Zussman, eds.). Proc. NATO Advanced Study Inst., Manchester Univ. Press, Manchester, England.
- & LALONDE, A. E. (1979): Turbidity in K-feldspars: causes and implications. *Geol. Soc. Amer. Program Abstr.* 11, 472-473.
- O'NEIL, J.R. & TAYLOR, H.P., JR. (1967): The oxygen isotope and cation exchange chemistry of feldspars. *Amer. Mineral.* 52, 1414-1437.
- ORLIAC, J. (1957): *Etude de la Pigmentation des Malgachites*. Mém. Dipl. Etudes Supérieures, Univ. Clermont-Ferrand, Clermont-Ferrand, France.
- PARSONS, I. (1978): Feldspars and fluids in cooling plutons. *Mineral. Mag.* 42, 1-17.

- (1980): Alkali-feldspar and Fe-Ti oxide exsolution textures as indicators of the distribution and subsolidus effects of magmatic "water" in the Klokken layered syenite intrusion, south Greenland. *Roy Soc. Edinb. Trans., Earth Sci.* 71, 1-12.
- SMITH, J.V. (1974): *Feldspar Minerals. 1. Crystal Structure and Physical Properties. 2. Chemical and Textural Properties.* Springer-Verlag, New York.
- STEWART, D.B. & WRIGHT, T.L. (1974): Al/Si order and symmetry of natural alkali feldspars, and the relationship of strained cell parameters to bulk composition. *Soc. franç. Minéral. Crist. Bull.* 97, 356-377.
- TAYLOR H.P., JR. (1968): The oxygen-isotope geochemistry of igneous rocks. *Contr. Mineral. Petrology* 19, 1-71.
- & FORESTER, R.W. (1979): An oxygen and hydrogen isotope study of the Skaergaard intrusion and its country rocks: a description of a 55-m.y.-old fossil hydrothermal system. *J. Petrology* 20, 355-419.
- YUND, R.A. (1974): Coherent exsolution in the alkali feldspars. In *Geochemical Transport and Kinetics* (A.W. Hoffman, B.J. Gilletti, H.S. Yoder, Jr. & R.A. Yund, eds.). *Carnegie Inst. Wash. Publ.* 634, 173-183.
- (1975): Subsidius phase relations in the alkali feldspars, with emphasis on coherent phases. In *Feldspar Mineralogy* (P.H. Ribbe, ed.). *Mineral. Soc. Amer. Short Course Notes* 2, Y1-28.
- & MCCALLISTER, R.H. (1970): Kinetics and mechanisms of exsolution. *Chem. Geol.* 6, 5-30.

Received May 29, 1982, revised manuscript accepted September 27, 1982.